The effect of pyrolysis conditions on the composition of Chinese Jimsar shale oil using FT-IR, ^{1}H-NMR and ^{13}C-NMR techniques

Hao Lu[a], Luwei Pan[a]*, Yue Guo[a]*, Fangqin Dai[a], Shaohui Pei[b,c], Jianning Huang[b,c], Shuang Liu[b]

[a] The State Key Laboratory of Refractories and Metallurgy, Wuhan University of Science and Technology, No.947 Heping Avenue, Qingshan District, Wuhan 430081, P. R. China
[b] Liaoning Chengda Co. Ltd., No.71 Renmin Road, Zhongshan District, Dalian 116000, P. R. China
[c] Xinjiang BaoMing Mines Co. Ltd., No.21 Wenhua Road, Jimsar 831700, P. R. China

Abstract. *Fourier transform infrared spectroscopy (FT-IR) and nuclear magnetic resonance (NMR) were used to characterize the functional groups and structural parameters of shale oil obtained from the pyrolysis of Chinese Jimsar oil shale under different process conditions: pyrolysis temperature 480, 500, 520, 550 °C, residence time 10, 20, 30, 40 min and heating rate 2, 5, 8, 10 °C/min. The results show that the main substances in shale oil are aliphatic components, mainly –CH$_2$ with antisymmetric stretching vibrations. The longest aliphatic chain of shale oil is at the pyrolysis temperature of 520 °C, the residence time of 20 min and the heating rate of 5 °C/min. The relative content of aromatics in shale oil is less than 20%. Di-substitution is the main substitution mode of the benzene ring, accounting for more than 45%. The results also indicate that the relative content of oxygen-containing functional groups (C–O and C=O) is much smaller than that of –CH$_2$ and –CH$_3$, while the relative content of C–O is higher than that of C=O functional groups. The increase of temperature, heating rate and residence time contributes to the formation of aromatic compounds.*

Keywords*: Jimsar shale oil, pyrolysis conditions, FT-IR, ^{1}H-NMR, ^{13}C-NMR.*

* Corresponding author: e-mails *panluwei@wust.edu.cn, guoyue@wust.edu.cn*

1. Introduction

Oil shale, a fine-grained sedimentary rock containing significant amounts of kerogen which can be converted into shale oil and combustible gas through retorting, is regarded as a valuable supplement and alternative to conventional oil, as a source of energy [1]. Up to the present time, oil shale has been used for retorting to yield shale oil [2–5] and for burning directly as a fuel to generate electricity or heat for many years [6–8]. China's oil shale resource has been estimated at about 978 billion tons, which can be converted to about 61 billion tons of shale oil [9]. The shale oil amount is equivalent to twice as much crude oil reserves. Therefore, oil shale is considered an important oil supplementary energy in China.

   Both shale oil and petroleum are rich in alkanes and aromatics. The difference is that shale oil contains more alkenes and some non-hydrocarbon components such as oxygen, nitrogen and sulfur. Retorting oil shale to yield oil is an important part of the comprehensive utilization of China's oil shale resources, which is evaluated by the yield and quality of shale oil as two key indexes. Therefore, in order to promote the further use of shale oil, its research is highly essential. Many scholars have studied the yield and quality of shale oil based on operating parameters such as final pyrolysis temperature [10–12], heating rate [13–16] and residence time [17, 18]. For example, Huang et al. [19] investigated the influence of heating rate on the matrix pyrolysis of kerogen in oil shale using thermogravimetry-mass spectrometry (TG-MS), and found that the olefin/alkane ratio increased as the heating rate increased. Huang et al. [20] reported that a significant amount of n-alkanes was converted into cycloalkanes and olefins by the secondary cracking reaction as the pyrolysis temperature increased from 485 °C to 590 °C, and there were formed oxygen-containing organic substances such as phenols, alcohols, esters and ketones in shale oil. Williams and Ahmad [21] reported that the production of shale oil increased first and then decreased with the increase of temperature, and concluded that the secondary cracking reaction was enhanced with the increase of pyrolysis temperature. Litster et al. [17] studied the influence of the residence time of shale particles (18–35 min) on the pyrolysis of Rundle oil shale, and reported that the residence time had no significant effect on the oil yield.

   With the development of modern physical analysis technology and instruments, the Fourier transform infrared (FT-IR) technology can be used to conduct qualitative and quantitative analysis of complex functional groups [22–24], and the nuclear magnetic resonance (NMR) technology can be adopted to analyze the molecular structure of complex organic compounds of shale oil [25–27]. Wang et al. [28] studied the functional groups of oil shale in different regions. Molina et al. [29] used ^{1}H and ^{13}C spectroscopy to study crude oil and recorded a series of average molecular structure parameters. Bansal et al. [30] used ^{1}H NMR spectrum to estimate the content of monocyclic and

polycyclic aromatic hydrocarbons in petroleum, and compared the calculation results with chromatographic analysis. The results showed that the error was very small, thus establishing a more accurate estimation of petroleum structure parameters.

However, little work has been done to study the effect of process conditions on the structure and properties of shale oil from the pyrolysis of oil shale. In view of the fact that shale oil contains a large number of unsaturated hydrocarbons and hybrid atom compounds, the influence of process conditions on its structure and properties is necessary to be investigated to ensure the oil's maximum and efficient extraction and provide a fundamental basis for raw oil refining.

Therefore, in this paper, FT-IR and NMR techniques were adopted to study the effects of different temperatures (480, 500, 520, 550 °C), heating rates (2, 5, 8, 10 °C/min) and residence times (10, 20, 30, 40 min) on the functional groups and structural parameters of shale oil generated from the pyrolysis of Jimsar oil shale of China.

2. Experimental

2.1. Oil shale sample

Oil shale samples were obtained from Shichanggou mine located in Jimsar city, Xinjiang Uygur Autonomous Region, northwestern China. The results of proximate analysis, ultimate analysis and Fischer assay of Jimsar oil shale are shown in Table 1. For experiments, oil shale was crushed and sieved to less than 0.15 mm and was dried in an 80 °C blast drying oven for 4 hours.

Shale oil was produced by retorting oil shale at different final temperatures (480, 500, 520, 550 °C), heating rates (2, 5, 8, 10 °C/min) and residence times (10, 20, 30, 40 min) using an aluminium retort. In each experiment, the weight of the oil shale sample was 50 g. As the heating rate was varied, the pyrolysis temperature and residence time were kept at 520 °C and 20 min, respectively. With the pyrolysis temperature varied, the heating rate and residence time were maintained at 5 °C/min and 20 min, respectively. While the residence time was varied, the heating rate and pyrolysis temperature were kept at 5 °C/min and 520 °C, respectively.

The components of Jimsar shale oil have been figured out in a previous research using GC-MS, as shown in Table 2 [31]. The main components of Jimsar shale oil are aliphatic hydrocarbons (n-paraffins and 1-olefins), aromatic hydrocarbons and heteroatom-containing compounds ranging from the number of carbon atoms C_6–C_{26}.

Table 1. Characteristics of Jimsar oil shale samples

Proximate analysis (ad)	Moisture	0.89
	Volatile matter	19.63
	Fixed carbon	2.49
	Ash	76.99
Ultimate analysis (d)	C	14.89
	H	2.04
	O	3.53
	N	0.40
	S	0.35
Fischer assay (d)	Shale oil	8.87
	Gas	2.46
	Water	2.45
	Spent shale	86.22

ad – air dried basis, d – dry basis

Table 2. The distribution of major constituents in shale oil [31]

Number	Compound	Percentage, %	Number	Compound	Percentage, %
1	Benzene	0.47	24	1-Tetradecene	2.39
2	1-Heptene	1.15	25	n-Tetradecane	2.19
3	n-Heptane	0.68	26	1-Pentadecene	1.84
4	Toluene	3.95	27	n-Pentadecane	1.96
5	1-Octene	3.05	28	1-Hexadecene	1.47
6	n-Octane	2.44	29	n-Hexadecane	1.62
7	Paraxylene	6.31	30	1-Heptadecene	1.17
8	1-Nonene	5.63	31	n-Heptadecane	1.49
9	n-Nonane	4.19	32	1-Octadecene	0.94
10	Mesitylene	4.90	33	n-Octadecane	1.30
11	$C_8H_{11}N$	1.50	34	1-Nonadecene	0.82

Table 2 (continued)

12	1-Decene	6.28	35	n-Nonadecane	1.45
13	n-Decane	0.22	36	1-Eicosene	1.23
14	n-Undecane	4.84	37	n-Eicosane	1.06
15	C9H9CL	1.05	38	1-Heneicosene	0.27
16	1-Undecene	5.60	39	n-Heneicosane	0.57
17	n-Undecane	4.67	40	C21H44O	0.25
18	C10H10	2.32	41	n-Docosane	0.75
19	1-Dodecene	4.29	42	C22H46O	0.09
20	n-Dodecane	4.91	43	n-Tricosane	0.39
21	1-Tridecene	3.32	44	n-Tetracosane	0.24
22	n-Tridecane	3.38	45	n-Pentacosane	0.22
23	C11H10	0.91	46	n-Hexacosane	0.23

2.2. FT-IR experiments

Attenuated total reflection Fourier transform infrared spectroscopy (ATR-FT-IR) was used to analyze the functional groups of shale oil under different pyrolysis conditions. The experimental spectrum was recorded between 4000 cm^{-1} and 600 cm^{-1}, and the spectral resolution was 4 cm^{-1}.

2.3. NMR experiments

The nuclear magnetic resonance (NMR) experiment was carried out on a Bruker AVANCE 400 MHz nuclear magnetic resonance spectrometer (Switzerland). The solvent used was deuterochloroform (CDCl$_3$), whereas the temperature was set to 25 °C. Resonance frequencies of ^{1}H NMR and ^{13}C NMR were 400.15 MHz and 100.62 MHz, respectively, while the spectral widths were 8 KHz and 24 KHz, respectively. The sampling times of ^{1}H NMR and ^{13}C NMR were respectively 64 and 800 sec.

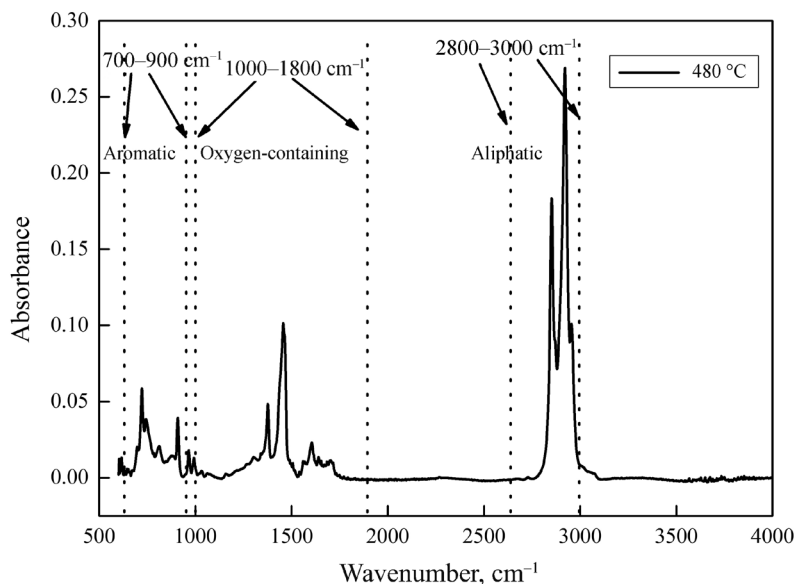## 3. Analysis of experimental results

3.1. FT-IR experiment

Fig. 1. FT-IR spectra of shale oil obtained at 480 °C, 5 °C/min and 20 min.

The spectral trends of shale oil are similar under different working conditions. Figure 1 shows the original FT-IR spectra of shale oil obtained at a final pyrolysis temperature of 480 °C. The FT-IR spectra of shale oil mainly include four regions: 3600–3000 cm^{-1}, 3000–2800 cm^{-1}, 1800–1000 cm^{-1} and 900–700 cm^{-1}, which are the characteristic peaks of the hydroxyl group, the aliphatic group, the oxygen-containing group and the aromatic structure, respectively. However, the hydroxyl functional group of 3600–3000 cm^{-1} was not noticeable in the FT-IR spectra of Jimsar shale oil and was therefore not analyzed in this work. The spectral curves of 3000–2800 cm^{-1}, 1800–1000 cm^{-1} and 900–700 cm^{-1} were fitted separately. In order to eliminate interference, baseline correction and curve smoothing were carried out before the spectral analysis of shale oil.

3.1.1. Analysis of the aliphatic group

The characteristic absorption peaks of the aliphatic group are in the range of 3000–2800 cm^{-1} with high absorption intensity. To make the fitted spectrum closer to the experimental spectrum, 8 peaks are fitted at 3000–2800 cm^{-1}. The correlation coefficients of all spectral fittings are larger than 0.99.

   Figure 2 shows the fitting spectrums of the aliphatic group in shale oil

obtained at different pyrolysis temperatures in the 3000–2800 cm^{-1} region. There are mainly four kinds of aliphatic substances in shale oil: methyl ($-CH_3$), methylene ($-CH_2$), methine ($-CH$) and methoxy ($-CHO$). The absorption peaks of $-CH_2$ are around 2851, 2919 and 2933 cm^{-1} in all the spectra [32]. The absorption peaks at 2851 cm^{-1} are the symmetric stretching vibration of $-CH_2$, while the other peaks are the antisymmetric stretching vibration of $-CH_2$ [33, 34]. The absorption peak around 2874 cm^{-1} is the symmetric stretching vibration of $-CH_3$ [34], while the peaks around 2955 and 2971 cm^{-1} are the antisymmetric stretching vibration of $-CH_3$. Jiang [35] reported that when the absorption peak of the $-CH_3$ antisymmetric stretching vibration in shale oil is at 2955 cm^{-1}, there is a certain number and considerable length of the long-chain aliphatic group in an orderly arrangement in shale oil. Additionally, the peaks around 2898 cm^{-1} and 2828 cm^{-1} represent the stretching vibrations of $-CH$ and $-CHO$, respectively.

(a)   (b)

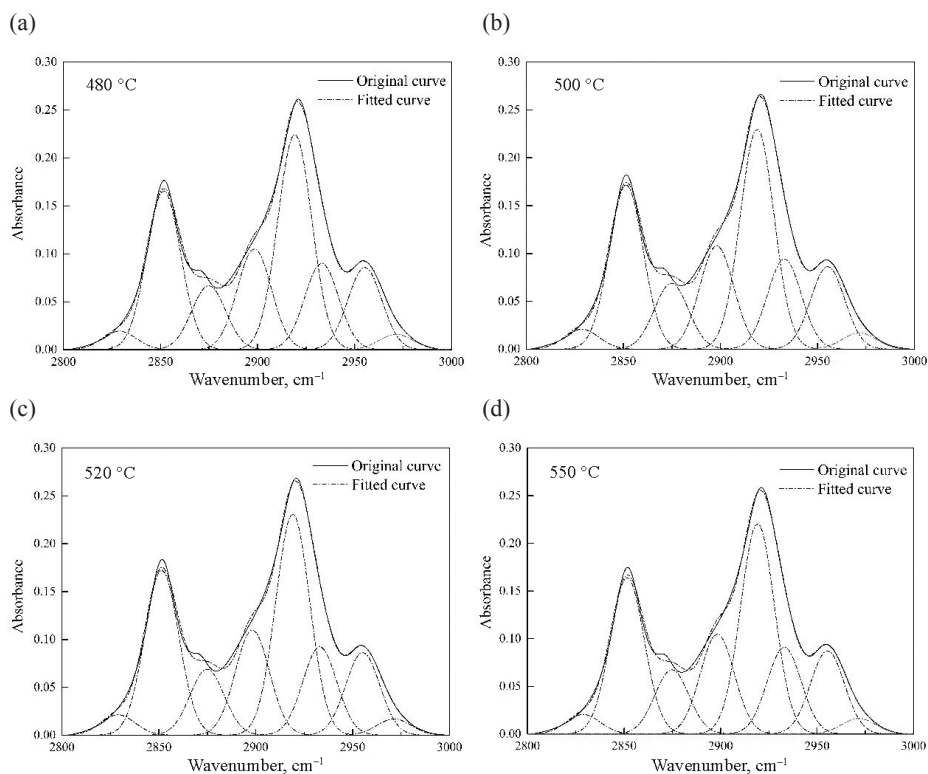(c)   (d)

Fig. 2. Curve fitting FT-IR spectra of the aliphatic group in shale oil obtained at the pyrolysis temperatures of (a) 480 °C, (b) 500 °C, (c) 520 °C, (d) 550 °C.

Table 3. Curve fitting analysis of the aliphatic C–H stretch band

Number	Assignment	Area percentage, %											
		Heating rate, °C/min				Residence time, min				Temperature, °C			
		2	5	8	10	10	20	30	40	480	500	520	550
1	–CHO	2.55	2.67	2.72	2.71	2.65	2.67	2.63	2.65	2.52	2.64	2.67	2.66
2	Sym. –CH_2	21.40	21.58	21.42	21.36	21.29	21.58	21.21	21.46	21.43	21.55	21.58	21.25
3	Sym. –CH_3	8.71	8.63	8.73	8.73	8.74	8.63	8.78	8.69	8.64	8.65	8.63	8.74
4	–R_3CH	13.54	13.74	13.55	13.50	1356	13.74	13.54	13.69	13.61	13.58	13.74	13.59
5	Asym. –CH_2	40.50	40.44	40.38	40.44	40.35	40.44	40.32	40.41	40.64	40.64	40.44	40.36
6	Asym. –CH_3	13.34	12.94	13.20	13.26	13.38	12.94	13.52	13.1	13.16	12.94	12.94	13.4
7	CH_2	61.90	62.02	61.8	61.8	61.64	62.02	61.53	61.87	62.07	62.19	62.02	61.61
8	CH_3	22.05	21.57	21.93	21.99	22.12	21.57	22.3	21.79	21.80	21.59	21.57	22.14
9	–CH_2/–CH_3	2.81	2.88	2.82	2.81	2.79	2.88	2.76	2.84	2.85	2.88	2.88	2.78

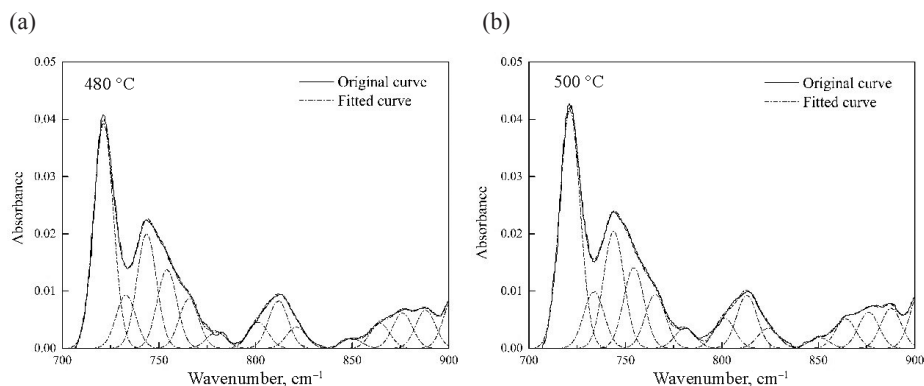Sym. – symmetric stretching vibration; Asym. – asymmetric stretching vibration

Table 3 gives the relative contents of functional groups corresponding to the fitting absorption peak of the aliphatic group in shale oil. The aliphatic component in all shale oil samples is mainly $-CH_2$, which accounts for about 60% of the entire aliphatic group. Of this the antisymmetric stretching vibration in the $-CH_2$ stretching vibration is twice the relative content of the symmetric stretching vibration. The aliphatic hydrogen of shale oil is dominated by methylene functional groups, as also reported by Wang et al. [28].

The effect of residence time on the relative content of the stretching vibration of $-CH_2$ and $-CH_3$ reveals no regularity in changes. As the heating rate increases, the stretching vibration of $-CH_2$ first increases and then decreases, while that of $-CH_3$ first decreases and thereafter increases. The effect of temperature and heating rate on the stretching vibration of $-CH_2$ is similar. The difference between $-CH_2$ and $-CH_3$ is that the stretching vibration of $-CH_3$ keeps decreasing with increasing temperature.

According to Wang et al. [28], the ratio between the absorption peak areas of $-CH_2$ and $-CH_3$ can reflect the length of aliphatic chains in the sample. Table 2 shows that the ratio of $-CH_2$ to $-CH_3$ increases firstly and then decreases with the increase of heating rate and temperature. The main reason is that, in the pyrolysis process, shale oil is secondarily cracked into gas at a higher heating rate and temperature. This explanation is augmented by the fact that oil obtained at high heating rates or temperatures contains less long-chain hydrocarbons [20, 36].

In addition, the residence time has no regularity effect on the ratio of $-CH_2$ to $-CH_3$. When the heating rate is 5 °C/min and the final temperature is 520 °C, the ratio of $-CH_2/-CH_3$ reaches the largest value, which indicates that shale oil has the longest aliphatic chain.

3.1.2. Analysis of the aromatic group

(a)   (b)

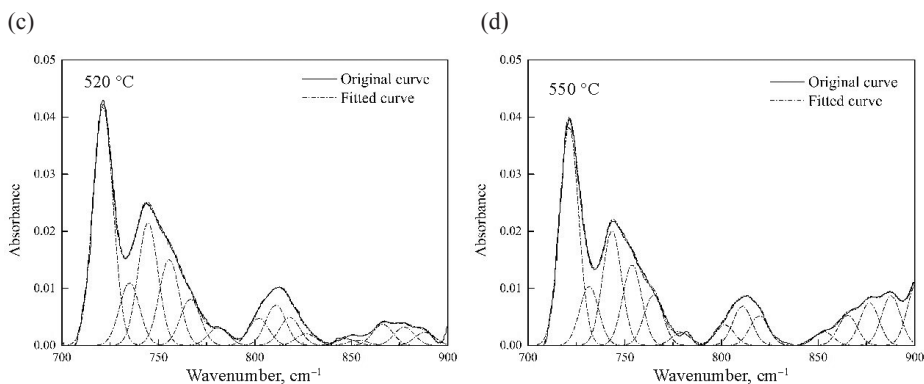(c)   (d)

Fig. 3. Curve fitting FT-IR spectra of the aromatic group in shale oil obtained at the pyrolysis temperatures of (a) 480 °C, (b) 500 °C, (c) 520 °C, (d) 550 °C.

The characteristic absorption peaks in the range of 900–700 cm^{-1} represent the C–H stretching vibration outside the aromatic plane. To make the fitted spectrum closer to the experimental spectrum, 14 peaks are fitted at 900–700 cm^{-1}. The correlation coefficients of all spectra fitting curves are larger than 0.99. Figure 3 shows the fitting spectrums of the aromatic group in shale oil obtained at different pyrolysis temperatures in the 900–700 cm^{-1} region. It can be seen from Figures 2 and 3 that the area of all peaks in the 900–700 cm^{-1} region in shale oil is much smaller than that in the 3000–2800 cm^{-1} region. This indicates that the content of aromatic compounds in shale oil is considerably smaller than that of aliphatic compounds. This is consistent with the results of a previous GC-MS experimental analysis of shale oil obtained by Pan et al. [31].

In the spectral range of 900–700 cm^{-1}, the C–H in the outside surface is mainly caused by the stretching vibration of the adjacent H deformation. The stretching vibration of the latter deformation mainly includes four kinds: benzene ring penta-substituted (900–860 cm^{-1}), benzene ring tetra-substituted (860–810 cm^{-1}), benzene ring tri-substituted (810–750 cm^{-1}) and benzene ring di-substituted (750–720 cm^{-1}). According to the above method, the relative contents of functional groups corresponding to the fitting absorption peak of the aromatic group in shale oil were calculated and are given in Table 4.

The substitution of the benzene ring is mainly di-substitution, which accounts for more than 45% of the entire aromatic group. This agrees with the value obtained by Wang et al. [28]. With increasing residence time and pyrolysis temperature, the di-substitution of the benzene ring increases firstly and then decreases, reaching a maximum value at a residence time of 30 min and temperature of 500 °C. However, the di-substitution mode will significantly decrease as the heating rate increases.

Additionally, Table 4 reveals that only the heating rate has an obvious effect on the tri-substitution and penta-substitution of the benzene ring. This

Table 4. Curve fitting analysis of the aromatic C–H group

Number	Benzene substitution	Area percentage, %											
		Heating rate, °C/min				Residence time, min				Temperature, °C			
		2	5	8	10	10	20	30	40	480	500	520	550
1	di-Substitution	50.62	49.3	48.66	45.69	48.03	49.3	49.61	48.12	49.98	50.23	49.3	47.81
2	tri-Substitution	19.54	21.1	20.47	20.13	20.78	21.1	18.44	21.5	21.77	22.66	21.1	20.06
3	tetra-Substitution	9.63	10.3	8.82	9.53	9.63	10.3	9.73	9.28	10.08	10.3	10.3	10.18
4	penta-Substitution	20.2	19.3	22.04	24.64	21.55	19.3	22.23	21.11	18.17	16.8	19.3	21.95

ring's tri-substitution increases firstly and then decreases with the heating rate increasing. At the same time, the changing trends of the penta-substitution of the benzene ring with heating rate are opposite to those of its tri-substitution. Furthermore, the relative content of the tetra-substitution of the benzene ring is the smallest in the four substitution modes. The effect of residence time and temperature on the tetra-substitution of the benzene ring is the same as that on its di-substitution. At the final temperature of 520 °C and residence time of 20 min, the ring's di-substitution reaches the highest value.

The results indicate that the substitution mode of the benzene ring is greatly affected by the parameters. This is because aromatic compounds are thermodynamically more stable than aliphatic compounds. Moreover, a variety of reactions concerning aromatic compounds will occur during the pyrolysis of oil shale when the process conditions change, including the gas phase cracking of aliphatic compounds to generate aromatic compounds, Diels-Alder type reactions resulting in the selective concentration of aromatic compounds, the aromatization reaction of cycloalkanes, etc. [37].

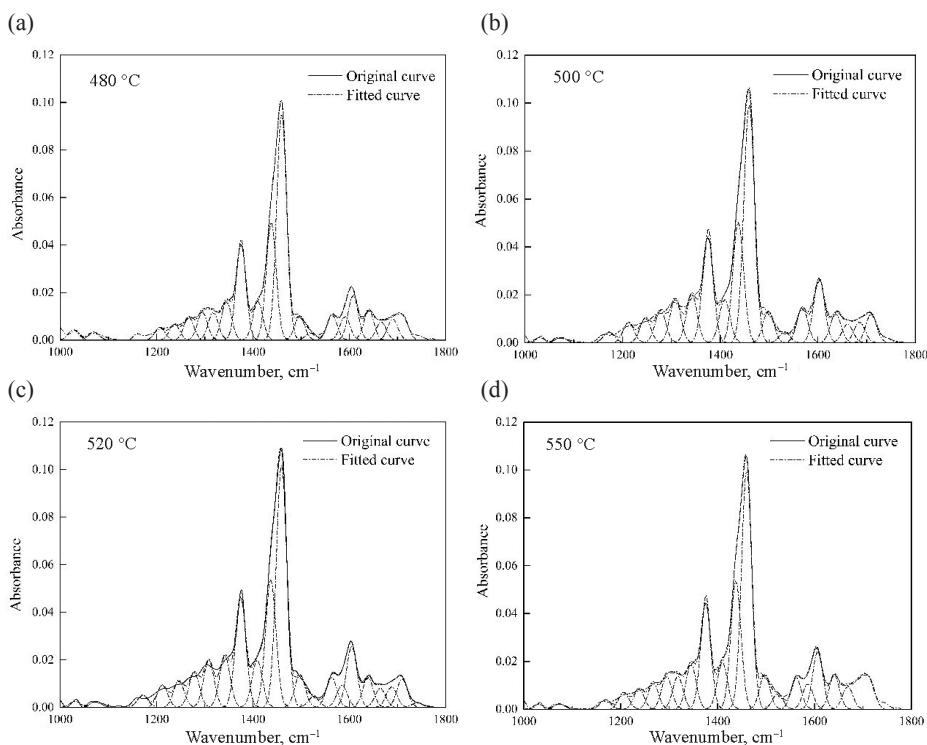### 3.1.3. Analysis of the oxygen-containing functional group

Fig. 4. Curve fitting FT-IR spectra of the oxygen-containing functional group in shale oil obtained at the pyrolysis temperatures of (a) 480 °C, (b) 500 °C, (c) 520 °C, (d) 550 °C.

The characteristic absorption peaks in the range of 1800–1000 cm^{-1} mainly represent the stretching vibration of oxygen-containing functional groups. 19 peaks are fitted in this region, and the correlation coefficients of all the fitted spectra exceeded 0.99. Figure 4 shows the fitting spectrums of the oxygenated group in shale oil obtained at different pyrolysis temperatures. In addition to C–O functional groups, shale oil also has a symmetrical deformation vibration of –CH$_3$ at 1375 cm^{-1} and an antisymmetric deformation vibration of –CH$_3$ or –CH$_2$ near 1460 cm^{-1}. Moreover, Painter et al. [38] reported that there were C=C stretching vibrations and conjugated C=O stretching vibrations in the 1700–1500 cm^{-1} region.

The relative contents of functional groups corresponding to the fitting absorption peak of oxygenated compounds in shale oil were calculated and are given in Table 5. Although the range of 1800–1000 cm^{-1} is an area containing oxygen functional groups, the –CH$_2$, –CH$_3$ and C=C functional groups also accounted for a large proportion. Especially high was the proportion of the antisymmetric deformation vibration of –CH$_3$ or –CH$_2$, surpassing 34%.

Compared with –CH$_2$, –CH$_3$ and C=C functional groups, the relative content of oxygen-containing functional groups (C–O and C=O) is comparatively small. However, Huang et al. [39] reported the oxygenated compounds to be the main component of non-hydrocarbons of shale oil. Moreover, Wang et al. [28] found that the relative content of C–O functional groups was much greater than that of C=O functional groups. The results presented by the researchers of the current work in Table 5 are consistent with those reported by Wang's group previously.

Tong et al. [40] reported that C=O structures were mainly quinones, ketones, esters, carboxylic acids and amides, while C–O structures were mainly alkyl and aryl ethers, alcohols, phenols and carbohydrates. In this article, oxygen-containing compounds mostly include ethers, acids, alcohols, phenols and esters. It can be seen from Table 5 that the oxidation-containing compounds are little affected by the process. This is because the proportion of oxygenated compounds in shale oil is determined by the maturity of oil shale [39]. Furthermore, some researchers [20] have found that oxygen-containing compounds are not stable when heated. This is mutually verified with the finding in the current article that oxygenated compounds first increase and then decrease with increasing residence time and temperature.

Different process conditions have different effects on oxygenated compounds. The C–O functional group first increases and then decreases with the increase of heating rate, while the C=O functional group is irregularly affected by the heating rate. Furthermore, the residence time has a similar effect on C–O and C=O functional groups, whereas both increase first and thereafter decrease. However, the effect of temperature on oxygen-containing functional groups is different from that of residence time. The C–O functional group first increased and then decreased with the increase of temperature, while the C=O functional group first decreased and then increased.

Table 5. Curve fitting analysis of shale oil at different operating parameters in the region 1800–1000 cm⁻¹

Number	Assignment	Area percentage, %															
		Heating rate, °C/min				Residence time, min					Temperature, °C					
		2	5	8	10	10	20	30	40	480	500	520	550
1	C–O	20.65	22.67	21.99	21.99	18.77	22.67	19.44	18.97	18.17	19.94	22.67	18.69
2	C=C	13.50	14.21	14.45	14.38	13.37	14.21	12.46	12.99	12.63	12.72	14.21	13.34
3	C=O	9.15	10.72	10.59	10.77	10.38	10.72	10.48	10.15	10.42	9.84	10.72	11.00
4	Sym. –CH₃	17.82	17.69	17.81	17.96	15.84	17.69	15.76	15.86	15.78	15.97	17.69	15.73
5	Asym. –CH₃, CH₂	38.88	34.71	35.16	34.9	41.64	34.71	41.86	42.03	43	41.53	34.71	41.24
6	C–O and C=O	29.80	33.39	32.58	32.76	29.15	33.39	29.92	29.12	28.59	29.78	33.39	29.69

Sym. – symmetric stretching vibration, Asym. – asymmetric stretching vibration

3.2. NMR experiment

The ^{1}H NMR and ^{13}C NMR spectra of shale oil produced from the pyrolysis of Jimsar oil shale under different process conditions are similar. Figure 5 shows these spectra of shale oil obtained at a pyrolysis temperature of 480 °C. The spectrum obtained from the experiment was analyzed using MestReNova 11.0 software. The chemical shift assignments of various types of hydrogen and carbon are given in Tables 6 and 7, respectively, based on literature data [41, 42].
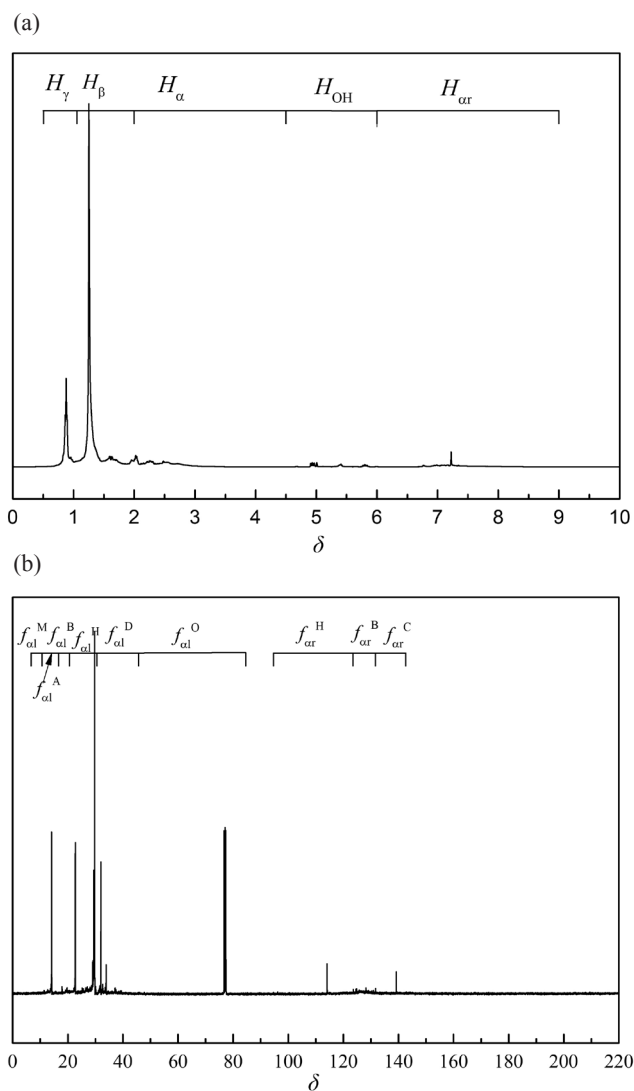
(a)

(b)

Fig. 5. ^{1}H NMR (a) and ^{13}C NMR (b) spectra of shale oil obtained at 480 °C, 5 °C/min and 20 min.

Table 6. Region division of ¹H NMR spectra [41, 42]

Symbol	Type of hydrogen	Chemical shift δ, ppm
H_γ	Aromatic ring γ-CH$_3$, cycloalkane methyl hydrogen	0.50–1.05
H_β	Aliphatic hydrogen β or further from aromatic ring	1.05–2.00
H_α	Aliphatic hydrogen α to aromatic ring (α-CH$_3$ or α-CH$_2$)	2.00–4.50
H_{OH}	Hydrogen connected to oxygen-containing group	4.50–6.0
$H_{\alpha r}$	Aromatic hydrogen	6.00–9.00

Table 7. Region division of ¹³C NMR spectra [41, 42]

Symbol	Type of carbon	Chemical shift δ, ppm
f_{al}^{M}	Methylic carbon	12.00–16.00
f_{al}^{A}	Aromatic carbon	16.00–22.00
f_{al}^{B}	Methylene carbon bonded to methyl	22.00–26.00
f_{al}^{H}	Methylene carbon	26.00–36.00
f_{al}^{D}	Methine, quaternary	36.00–51.00
f_{al}^{O}	Aliphatic carbon bonded to oxy-aromatic	51.00–90.00
f_{ar}^{H}	Protonated aromatic carbon	100.00–129.00
f_{ar}^{B}	Aromatic bridgehead carbon	129.00–137.00
f_{ar}^{C}	Aromatic branched carbon	137.00–148.00

3.2.1 ¹H MNR analysis of shale oil

As shown in Figure 5(a) and Table 8, the main resonance region of the hydrogen spectrum of shale oil is in the range of $\delta = 0.50–6.00$. In addition to the various types of hydrogen of α, β, and γ of the side chains of the aromatic ring, in this region there are also present different hydrogen types that are attached to oxygen-containing groups.

The $\delta = 1.05–2.00$ region is the main peak of the ¹H NMR spectra of shale oil. The hydrogen in this area is mainly aliphatic hydrogen β or further from the aromatic ring. Its content is greater than 60% in all shale oil samples.

Simultaneously, the relative content of the area of $\delta = 0.50–1.05$ is comparatively high, being about one-third of H_β. It was the resonance region of the aromatic ring γ-CH$_3$ or cycloalkane methyl hydrogen. The types of hydrogen in the 2.00–4.50 region are –CH$_3$ and –CH$_2$ at the α position of the side chain of the aromatic ring. The range of 4.50 to 6.0 ppm indicates hydrogen connected to the oxygen-containing group. Moreover, the hydrogen in the 6.00–9.00 region is the one with the aromatic rings. The hydrogen content in shale oil in this region is much lower than that in the region of 0.50–6.00. This indicates that the aromatic hydrogen content (H_{ar}) in shale oil is low. Wang et al. [43] also report that the aromatic hydrogen content in the heavy oil fraction of shale oil (shale oil boiling point > 300 °C) is very small.

Table 8. Hydrogen distribution in ^{1}H NMR spectra

Symbol	Relative content, %*											
	Heating rate, °C/min				Residence time, min				Temperature, °C			
	2	5	8	10	10	20	30	40	480	500	520	550
H_γ	16.86	16.83	16.39	16.10	16.23	16.83	16.44	16.64	16.69	17.06	16.83	16.34
H_β	63.68	62.95	62.47	62.17	62.74	62.95	62.77	63.49	63.86	63.48	62.95	63.36
H_α	10.70	10.90	11.28	11.62	11.65	10.90	11.48	10.90	10.64	10.53	10.90	11.17
H_{OH}	2.70	3.21	3.17	3.28	2.86	3.21	2.90	2.83	2.94	3.00	3.21	2.87
H_{ar}	6.03	6.11	6.69	6.83	6.52	6.11	6.41	6.14	5.86	5.93	6.11	6.27

* The ratio of the integral area of the corresponding spectrum area to the total area of the spectrum

Table 8 reveals that different process conditions have different effects on hydrogen distribution. The residence time only has an effect on H_{OH}. That is, H_{OH} increases first and then decreases as the residence time increases. The H_{OH} value reaches the maximum value of 3.208% when the residence time is 20 min. The decrease in H_{OH} may be caused by a secondary reaction in the retort to generate shale gas or shale carbon as the residence time increases.

The heating rate has no obvious influence on H_{OH}, but it has a great influence on the distribution of other types of hydrogen in shale oil. Among them, H_γ and H_β keep decreasing as the heating rate increases, while H_α and H_{ar} keep increasing. This is because the increase in the heating rate is conducive to the pyrolysis of oil shale and facilitates the increase of light fractions in shale oil [37]. Moreover, Nazzal [44] reported that aromatic compounds increased with the heating rate increasing from 2 to 30 °C/min. These results verify the effect of heating rate on hydrogen distribution in shale oil.

In addition, temperature also has a great influence on the distribution of hydrogen in shale oil. The effect of temperature on H_β and H_{ar} is mostly similar to that of heating rate. The difference is that H_γ first increases and then decreases with the increase of temperature, reaching a maximum value at 500 °C. Additionally, the influence of temperature on H_α is opposite to that on H_γ. However, Wang et al. [28] reported that the C–C bond of the saturated hydrocarbon group attached to the aromatic ring broke as the pyrolysis temperature increased from 400 °C to 600 °C, and caused H_α and H_{ar} to gradually increase and H_β to gradually decrease in the heavy oil fraction of shale oil. At the same time, the researchers also reported that the content of H_γ would not change systematically with the increase in the final pyrolysis temperature. That is why they were looking at heavy oil fractions of shale oil. Wang et al. [45] reported that the heavy fractions in shale oil firstly decreased with increasing temperature (430, 460, 490, 520 °C) from 430 °C to 490 °C, and then increased as the temperature was higher than 490 °C. Therefore, the results obtained in this paper are principally similar to those of Wang et al. [28], but not exactly the same.

Table 9. Distribution of carbon in ^{13}C NMR spectra

Symbol	Relative content, %*											
	Heating rate, °C/min				Residence time, min				Temperature, °C			
	2	5	8	10	10	20	30	40	480	500	520	550
f_{al}^{M}	10.47	9.00	6.48	6.87	10.29	9.00	7.65	9.58	9.75	9.99	9.00	8.71
f_{al}^{A}	7.30	5.00	4.00	5.06	6.29	5.00	5.89	6.24	5.16	6.59	5.00	5.81
f_{al}^{B}	11.34	10.00	7.47	7.81	12.00	10.00	8.36	10.98	11.02	11.17	10.00	9.97
f_{al}^{H}	52.82	51.50	47.64	42.93	57.14	51.50	42.35	52.73	54.64	52.52	51.50	49.05
f_{al}^{D}	4.63	6.50	5.28	6.11	1.14	6.50	5.46	4.83	5.34	5.22	6.50	4.55
f_{al}^{O}	8.78	1.50	8.55	10.04	4.57	1.50	10.00	2.16	8.43	2.20	1.50	6.55
f_{ar}^{H}	0.77	7.00	11.67	12.70	3.43	7.00	12.18	6.67	1.71	5.32	7.00	6.26
f_{ar}^{B}	2.843	5.00	4.76	4.60	3.43	5.00	4.37	4.33	2.82	4.35	5.00	4.84
f_{ar}^{C}	1.054	3.50	4.16	3.89	1.71	3.50	3.74	2.49	1.13	2.65	3.50	3.90

* The ratio of the integral area of the corresponding spectrum area to the total area of the spectrum

3.2.2. Structural parameters of shale oil calculated by ^{1}H MNR and ^{13}C MNR

The chemical shift of the ^{13}C NMR spectrum of shale oil is mainly divided into the aliphatic carbon region (< 90) and the aromatic carbon region (> 100). As shown in Figure 5b and Table 9, the chemical shift of the ^{13}C NMR spectrum of shale oil generated under different process conditions has the main resonance region at $\delta < 90$. The resonance of the methylene carbon region ($\delta = 26.00–36.00$) is the strongest, with the relative content of more than 42%. The resonance intensity of the corresponding terminal methyl carbon ($\delta = 8–16$) is relatively weak. At the same time, the resonance intensity of the chemical shift greater than $\delta > 100$ is not obvious. This implies that shale oil contains less aromatics.

Table 10. Hydrocarbon types and their structural parameters

Structural parameter	Symbol	Definition
Ratio of aromatic carbon	f_a	$f_a = f_{ar}^H + f_{ar}^B + f_{ar}^C$
Ratio of aliphatic carbon	f_{al}	$f_{al} = f_{al}^M + f_{al}^A + f_{al}^B + f_{al}^H + f_{al}^D + f_{al}^O$
Average carbon number of substituents	N	$N = (H_{\alpha} + H_{\beta} + H_{\gamma})/H_{\alpha}$
Unsubstituted aromatic ring hydrogen to aromatic carbon ratio	Q	$Q = (H_{\alpha} + H_{\beta})/2f_{\alpha}$

In order to further analyze the molecular structure of shale oil, hydrocarbon types and structural parameters in it are characterized according to the structural parameters of hydrogen and carbon spectra. The characterization formula is presented in Table 10, the calculation results are given in Table 11. The results show that the relative content of aromatic carbon (f_a) in the Jimsar shale oil is much lower than that of aliphatic carbon (f_{al}). This is consistent with the results of analysis presented above. Additionally, it was found that with the increase of process parameters, the relative content of aromatic carbon increased. However, the relative content of aromatic carbon decreased as a process parameter increased. Some researchers believed that this is due to some secondary reactions in the pyrolysis process of shale oil. The increase of aromatic carbon may be due the gas phase cracking of aliphatic compounds to generate aromatic compounds, Diels-Alder type reactions resulting in the selective concentration of aromatic compounds and the aromatization reaction of cycloalkanes [37, 44, 45]. The reduction of aromatic carbon is due to the coke reaction of aromatics during pyrolysis.

Table 11. Hydrocarbon types and their structural parameters calculated

Symbol	Value											
	Temperature, °C				Heating rate, °C/min				Residence time, min			
	480	500	520	550	2	5	8	10	10	20	30	40
f_a	0.05	0.12	0.16	0.15	0.05	0.16	0.21	0.21	0.09	0.16	0.20	0.14
f_{al}	0.94	0.88	0.84	0.85	0.95	0.84	0.69	0.72	0.91	0.84	0.75	0.87
N	8.97	9.06	8.66	8.54	8.95	8.66	8.37	8.12	8.30	8.66	8.37	8.73
Q	6.53	2.98	2.37	2.46	7.90	2.37	1.78	1.73	4.291	2.37	1.81	2.74

Wang et al. [28] believed the properties of shale oil to be similar to coal tar's. The average carbon number (N) of substituted alkyl groups in shale oil is related to the maturity of oil shale. Moreover, N signifies that hydrocarbons are mainly derived from the cracking of long-chain hydrocarbons or alkyl chains. Compared with coal tar, shale oil has a longer side chain. Table 11 shows that N increases firstly and then decreases with increasing temperature, while with the increase of heating rate it also increases. These results demonstrate that the pyrolysis of shale oil involves a secondary reaction.

The condensation index (Q) refers to the ratio of unsubstituted aromatic ring hydrogen to aromatic carbon. Q firstly decreases and then increases with temperature and residence time increasing, while with the increase of heating rate it decreases. As the temperature, heating rate and residence time are the smallest, the value of Q is the highest, indicating that the unsubstituted aromatic ring contains more hydrogen. These results show that the increase in temperature, heating rate and residence time is conducive to the formation of aromatic compounds. At the temperature of 520 °C, the residence time of 20 min and the heating rate of 10 °C/min, the value of Q is the smallest, which is more conducive to the formation of aromatic compounds. There are many researchers who are also of the opinion that the increase in heating rate, residence time and temperature within a certain range contributes the formation of aromatic compounds [37, 44, 45].

4. Conclusions

1. The FTIR, ^{1}H NMR and ^{13}C NMR analyses indicate that the main substances in shale oil are aliphatic components. FTIR results show that the aliphatic components in shale oil samples are mainly –CH$_2$ with anti-symmetric stretching vibrations, which decrease firstly and then increase with the increase

of heating rate, and decrease with the increase of temperature. Shale oil has the longest aliphatic chain at the following pyrolysis conditions: heating rate 5 °C/min, pyrolysis temperature 520 °C and residence time 20 min.

2. The di-substitution is the main substitution mode of the benzene ring, accounting for more than 45%. The di-substitution of the benzene ring increases firstly and then decreases with increasing residence time and temperature, and decreases with the increase of heating rate. The results of ^{1}H NMR and ^{13}C NMR also show the relative content of aromatics in shale oil to be less than 20%. The increase of temperature, heating rate and residence time is conducive to the formation of aromatic compounds.

3. The relative content of oxygen-containing functional groups C–O and C=O is much smaller than that of –CH$_2$ and –CH$_3$ functional groups, while the relative content of C–O is greater than that of C=O. The relative content of C–O functional groups firstly increases and then decreases with the increase of heating rate, residence time and temperature. The relative content of C=O functional groups firstly increases and then decreases with the increase of residence time, while the temperature firstly increases, then decreases and thereafter increases again.

Acknowledgements

REFERENCES

1. Mozaffari, P., Baird, Z. S., Listak, M., Oja, V. Vapor pressures of narrow gasoline fractions of oil from industrial retorting of Kukersite oil shale. *Oil Shale*, 2020, **37**(4), 288–303.
2. Kairbekov, Z. K., Masuda, N., Ohshima, M. A., Myltykbaeva, Z. K., Kairbayeva, N., Yemilyanova, V. S., Kurokawa, H., Miura, H. Preliminary analysis of oil shale obtained from Kalynkara in Kazakhstan. *J. Japan. Pet. Inst.*, 2014, **57**(4), 192–195.
3. Dong, R. T., Xia, L. Z., Wang, H. N., Jiao, D. S. 3-D CFD simulation of oil shale drying in fluidized bed and experimental verification. *Oil Shale*, 2020, **37**(4), 334–356.
4. Bai, J. R., Bai, Z., Li, S. Y., Wang, Q. Process simulation of oil shale comprehensive utilization system based on Huadian-type retorting technique. *Oil Shale*, 2015, **32**(1), 66–81.
5. Yue, C. T., Liu, Y., Ma, Y., Li, S. Y., He, J. L., Qiu, D. K. Influence of retorting conditions on the pyrolysis of Yaojie oil shale. *Oil Shale*, 2014, **31**(1), 66–78.

6.   Azzam, S. M. *The Combustion of Low Calorific Value Fuels Using a Fluidized Bed Combustor*. M.Sc. Thesis, Mech. Eng. Dept., Jordan University of Science and Technology, Irbid, 1993.

7.   Hotta, A., Parkkonen, R., Hiltunen, M., Arro, H., Loosaar, J., Parve, T., Pihu, T., Prikk, A., Tiikma, T. Experience of Estonian oil shale combustion based on CFB technology at Narva Power Plants. *Oil Shale*, 2005, **22**(4), 381–397.

8.   Sidorkin, V. T., Tugov, A. N., Vereshchetin, V. A., Mel'nikov, D. A. Assessment of combustion of oil shale refinery by-products in a TP-101 boiler. *Therm. eng. (Toukyou. Online)*, 2015, **62**(4), 271–277.

9.   Liu, Z. J., Meng, Q. T., Dong, Q. S., Zhu, J. W., Guo, W., Ye, S. Q, Liu, R., Jia, J. Characteristics and resource potential of oil shale in China. *Oil Shale,* 2017, **34**(1), 15–41.

10. Zhang, Y., Han, Z. N., Wu, H., Lai, D. G., Glarborg, P., Xu, G. W. Interactive matching between the temperature profile and secondary reactions of oil shale pyrolysis. *Energy Fuels*, 2016, **30**(4), 2865–2873.

11. Wang, W., Ma, Y., Li, S., Shi, J., Teng, J. Effect of temperature on the EPR properties of oil shale pyrolysates. *Energy Fuels*, 2016, **30**(2), 830–834.

12. Nguimbi, G. R., Sun, Y., Guo, M., Bolou, D. B., Ondon, B. S., Cryton, P. Pyrolysis and evaluation of oil shale product yield and composition from Tchikatanga-Makola (Congo) oil shale. *Int. Energy J.*, 2016, **16**(1), 37–45.

13. Siramard, S., Bunman, Y., Lai, D., Xu, G. Pyrolysis of Huadian oil shale in an infrared heating reactor. *Energy Fuels*, 2017, **31**(7), 6996–7003.

14. Kaljuvee, T., Štubňa, I., Húlan, T., Kuusik, R. Heating rate effect on the thermal behavior of some clays and their blends with oil shale ash additives. *J. Therm. Anal. Calorim.*, 2016, **127**(1), 33–45.

15. Lin, L. X., Lai, D. G., Guo, E., Zhang, C., Xu, G. W. Oil shale pyrolysis in indirectly heated fixed bed with metallic plates of heating enhancement. *Fuel*, 2016, **163**, 48–55.

16. Liang, K., Liang, J., Shi, L., Ma, G., Wang, L., Wang, J., Liang, P. Effects of heating rate on the pyrolysis characteristics and kinetics of Huadian oil shale. *Journal of Mining Science and Technology*, 2018, **3**(2), 194–200 (in Chinese).

17. Litster, J. D., Newell, R. B., Bell, P. R. F. Pyrolysis of Rundle oil shale in a continuous fluidized bed retort. *Fuel*, 1988, **67**(10), 1327–1330.

18. Nazzal, J. M., The influence of grain size on the products yield and shale oil composition from the pyrolysis of Sultani oil shale. *Energ. Convers. Manag.*, 2008, **49**(11), 3278–3286.

19. Huang, Y. R., Fan, C., Han, X. X., Jiang, X. M. A TGA-MS investigation of the effect of heating rate and mineral matrix on the pyrolysis of kerogen in oil shale, *Oil Shale*, 2016, **33**(2), 125–141.

20. Huang, Y. R., Han, X. X., Jiang, X. M. Comparison of fast pyrolysis characteristics of Huadian oil shales from different mines using Curie-point pyrolysis-GC/MS. *Fuel Process. Technol.*, 2014, **128**, 456–460.

21. Williams, P. T., Ahmad, N. Influence of process conditions on the pyrolysis of Pakistani oil shales. *Fuel*, 1999, **78**(6), 653–662.

22. Xiao, G. D., Dong, D. M., Liao, T. Q., Li, Y., Zheng, L., Zhang, D. Y., Zhao, C. J. Detection of pesticide (Chlorpyrifos) residues on fruit peels through spectra of volatiles by FTIR. *Food Anal. Methods*, 2015, **8**(5), 1341–1346.

23. Szymanska-Chargot, M., Chylinska, M., Kruk, B., Zdunek, A. Combining FT-IR spectroscopy and multivariate analysis for qualitative and quantitative analysis of the cell wall composition changes during apples development. *Carbohydr. Polym.*, 2015, **115**, 93–103.

24. Magerman, C. M. *The Evaluation of Fourier Transform Infrared (FT-IR) Spectroscopy for Quantitative and Qualitative Monitoring of Alcoholic Wine Fermentation*. M.Sc. Thesis, Stellenbosch University, 2009.

25. Chamberlain, N. F. Determining molecular structure by nuclear magnetic resonance of hydrogen. *Analytical Chemistry*, 1959, **31**(1), 56–77.

26. Becker, E. D., Fisk, C. L. NMR: New techniques for chemical analysis and biological investigation. In: *Research Instrumentation for the 21st Century* (Beecher, G. R., ed.). Springer Netherlands, 1988, 269–291.

27. Jackson, R. L., Strange, J. H. Molecular motion in the plastic phase of pivalic acid studied by nuclear magnetic resonance. *Mol. Phys.*, 1971, **22**(2), 313–323.

28. Wang, Q., Cui, D., Wang, P., Bai, J. R., Wang, Z. C., Liu, B. A comparison of the structures of >300 °C fractions in six Chinese shale oils obtained from different locations using ^{1}H NMR, ^{13}C NMR and FT-IR analyses. *Fuel*, 2018, **211**, 341–352.

29. Molina, V. D., Ariza, E., Poveda, J. C. Structural differences among the asphaltenes in Colombian light crudes from the Colorado Oil field. *Energy Fuels*, 2017, **31**(1), 133–139.

30. Bansal, V., Krishna, G. J., Singh, A. P., Gupta, A. K., Sarpal, A. S. Determination of Hydrocarbons Types and Oxygenates in Motor Gasoline: A Comparative Study by Different Analytical Techniques. *Energy Fuels*, 2008, **22**(1), 410–415.

31. Pan, L. W., Dai, F. Q., Pei, S. H., Huang, J. N., Liu, S. Influence of particle size and temperature on the yield and composition of products from the pyrolysis of Jimsar (China) oil shale. *J. Anal. Appl. Pyrolysis*, 2021, **157**, 105211.

32. Bruan, V., Halim, M., Ziyad, M., Largeau, C., Amblès, A. Characterization of the Moroccan Timahdit (X-layer) oil shale kerogen using pyrolysis and thermally assisted hydrolysis and methylation. *J. Anal. Appl. Pyrolysis*, 2001, **61**(1), 165–179.

33. Ma, Y. H., Zhu, J. X., He, H. P., Yuan, P., Shen, W., Liu, D. Infrared investigation of organo-montmorillonites prepared from different surfactants. *Spectrochim. Acta A.*, 2010, **76**(2), 122–129.

34. Guo, Y., Wu, P. FTIR spectroscopic study of the acrylamide states in AOT reversed micelles. *J. Mol. Struct.*, 2008, **883**–**884**, 31–37.

35. Jiang, H. B. *Experimental study on low temperature pyrolysis process of oil shale and key components of circulating fluidized bed*. 2016 (in Chinese).

36. Al-Harahsheh, A., Al-Ayed, O., Al-Harahsheh, M., Abu-El-Halawah, R. Heating rate effect on fractional yield and composition of oil retorted from El-lajjun oil shale. *J. Anal. Appl. Pyrolysis*, 2010, **89**(2), 239–243.

37. Wang, S., Liu, J. G., Jiang, X. M., Han, X. X., Tong, J. H. Effect of heating rate on products yield and characteristics of non-condensable gases and shale oil obtained by retorting Dachengzi oil shale. *Oil Shale*, 2013, **30**(1), 27–47.

38. Painter, P. C., Snyder, R. W., Starsinic, M., Coleman, M. M., Kuehn, D. W., Davis, A. Concerning the application of FT-IR to the study of Coal: A critical assessment of band assignments and the application of spectral analysis programs. *Appl. Spectrosc.*, 1981, **35**(5), 475–485.

39. Huang, Y. R., Han, X. X., Jiang, X. M. Characterization of Dachengzi oil shale fast pyrolysis by Curie-point pyrolysis-GC-MS. *Oil Shale*, 2015, **32**(2), 134–150.

40. Tong, J. H., Han, X. X., Wang, S., Jiang, X. M. Evaluation of structural characteristics of Huadian oil shale kerogen using direct techniques (solid-state ^{13}C NMR, XPS, FT-IR, and XRD). *Energy Fuel*s, 2011, **25**(9), 4006–4013.

41. Chi, M. S., Wang, Q., Shi, J. X., Liu, Q., Cui, D., Pan, S. 1H nuclear magnetic resonance-based chemical structure characteristics analysis of Huadian shale oil. *Science Technology and Engineering*, 2018, **18**(11), 82–88 (in Chinese).

42. Wang, Q., Ge, J. X., Jia, C. X., Xu, X. F., Liu, H. P. Influence of retorting end temperature on chemical structure of oil-sand oil. *CIESC Journal*, 2013, **64**(11), 4216–4222 (in Chinese).

43. Wang, Q., Cui, D., Chi, M. S., Zhang, H. X., Xu, X. C. Influence of final retorting temperature on composition and property of Huadian shale oil. *CIESC Journal*, 2015, **66**(7), 2670–2677 (in Chinese).

44. Nazzal, J. M. Influence of heating rate on the pyrolysis of Jordan oil shale. *J. Anal. Appl. Pyrolysis*, 2002, **62**(2), 225–238.

45. Wang, S, Jiang, X. M., Han, X. X., Tong, J. H. Effect of retorting temperature on product yield and characteristics of non-condensable gases and shale oil obtained by retorting Huadian oil shales. *Fuel Process. Technol.*, 2014, **121**, 9–15.